Understanding Deep Learning

Chapter 18: Diffusion models

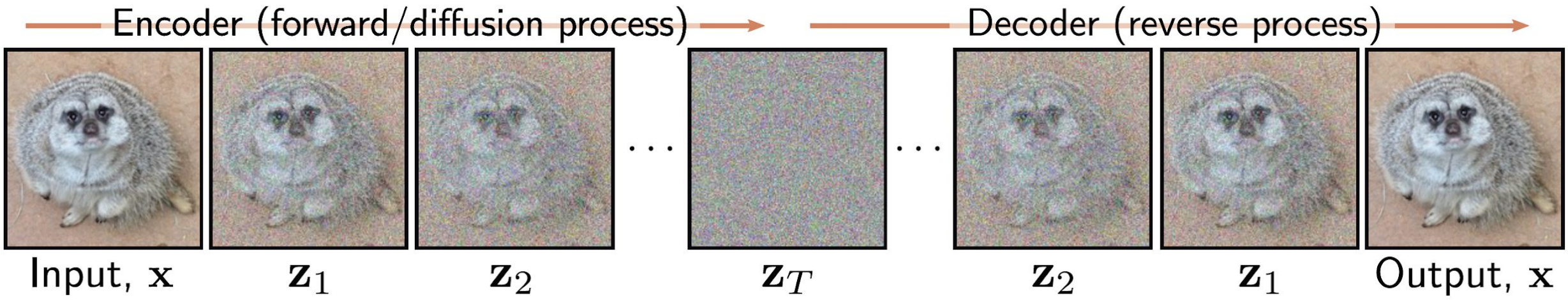

Figure 18.1 Diffusion models. The encoder (forward, or diffusion process) maps the input $\mathbf{x}$ through a series of latent variables $\mathbf{z}_1 \ldots \mathbf{z}_T$. This process is pre-specified and gradually mixes the data with noise until only noise remains. The decoder (reverse process) is learned and passes the data back through the latent variables, removing noise at each stage. After training, new examples are generated by sampling noise vectors $\mathbf{z}_T$ and passing them through the decoder.

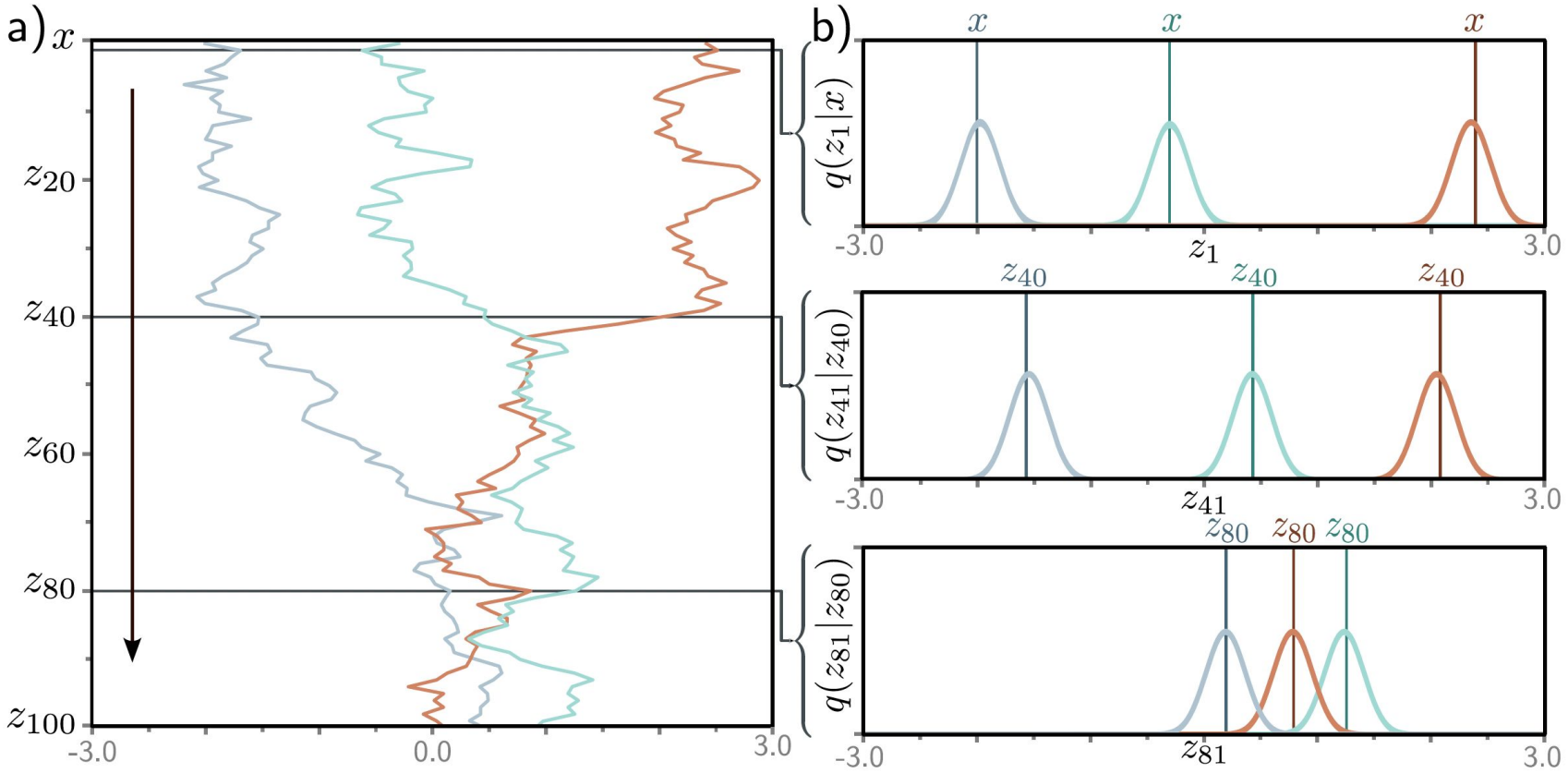

Figure 18.2 Forward process. a) We consider one-dimensional data x with $T = 100$ latent variables $z_1, \ldots, z_{100}$ and $\beta = 0.03$ at all steps. Three values of x (orange, green, and gray) are initialized (top row). These are propagated through $z_1, \ldots, z_{100}$. At each step, the variable is updated by attenuating its value by $\sqrt{1-\beta}$ and adding noise with mean zero and variance β (equation 18.1). Accordingly, the three examples noisily propagate through the variables with a tendency to move toward zero. b) The conditional probabilities $Pr(z_1|x)$ and $Pr(z_t|z_{t-1})$ are normal distributions with a mean that is slightly closer to zero than the current point and a fixed variance β_t (equation 18.2).

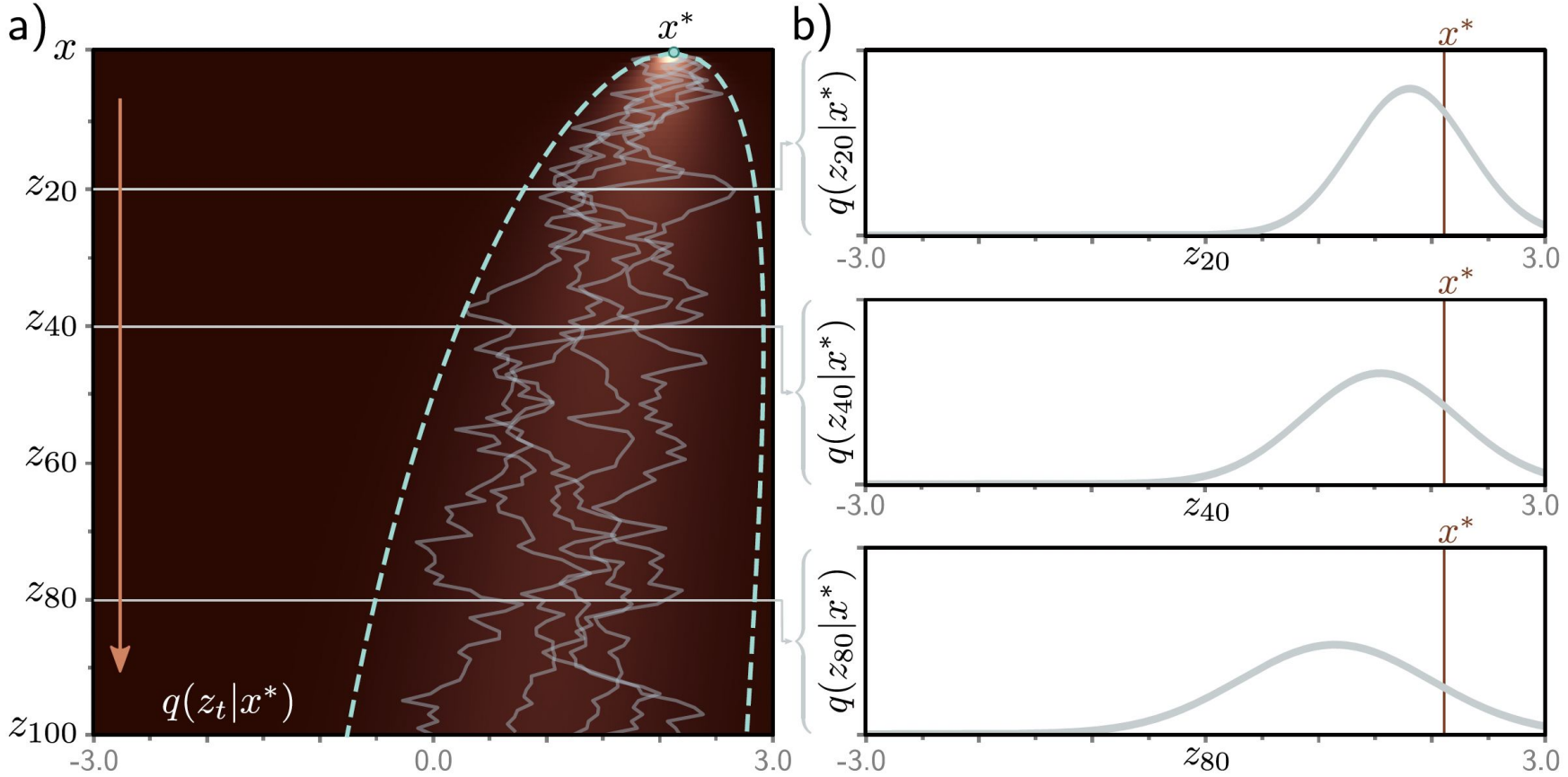

Figure 18.3 Diffusion kernel. a) The point $x^* = 2.0$ is propagated through the latent variables using equation 18.1 (five paths shown in gray). The diffusion kernel $q(z_t|x^*)$ is the probability distribution over variable z_t given that we started from x^*. It can be computed in closed-form and is a normal distribution whose mean moves toward zero and whose variance increases as t increases. Heatmap shows $q(z_t|x^*)$ for each variable. Cyan lines show ± 2 standard deviations from the mean. b) The diffusion kernel $q(z_t|x^*)$ is shown explicitly for $t = 20, 40, 80$. In practice, the diffusion kernel allows us to sample a latent variable z_t corresponding to a given x^* without computing the intermediate variables $z_1, \ldots, z_{t-1}$. When t becomes very large, the diffusion kernel becomes a standard normal.

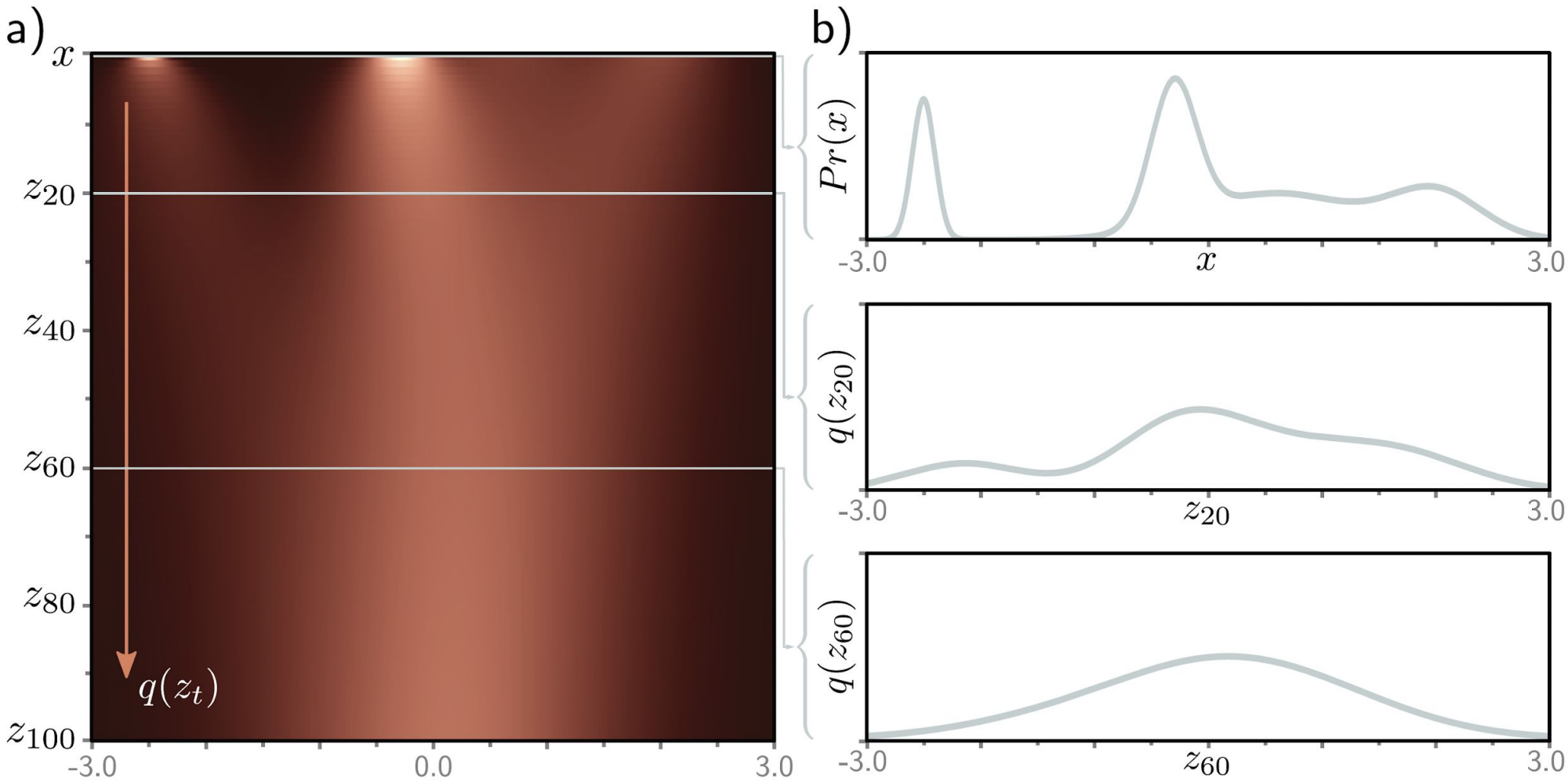

Figure 18.4 Marginal distributions. a) Given an initial density $Pr(x)$ (top row), the diffusion process gradually blurs the distribution as it passes through the latent variables z_t and moves it toward a standard normal distribution. Each subsequent horizontal line of heatmap represents a marginal distribution $q(z_t)$. b) The top graph shows the initial distribution $Pr(x)$. The other two graphs show the marginal distributions $q(z_{20})$ and $q(z_{60})$, respectively.

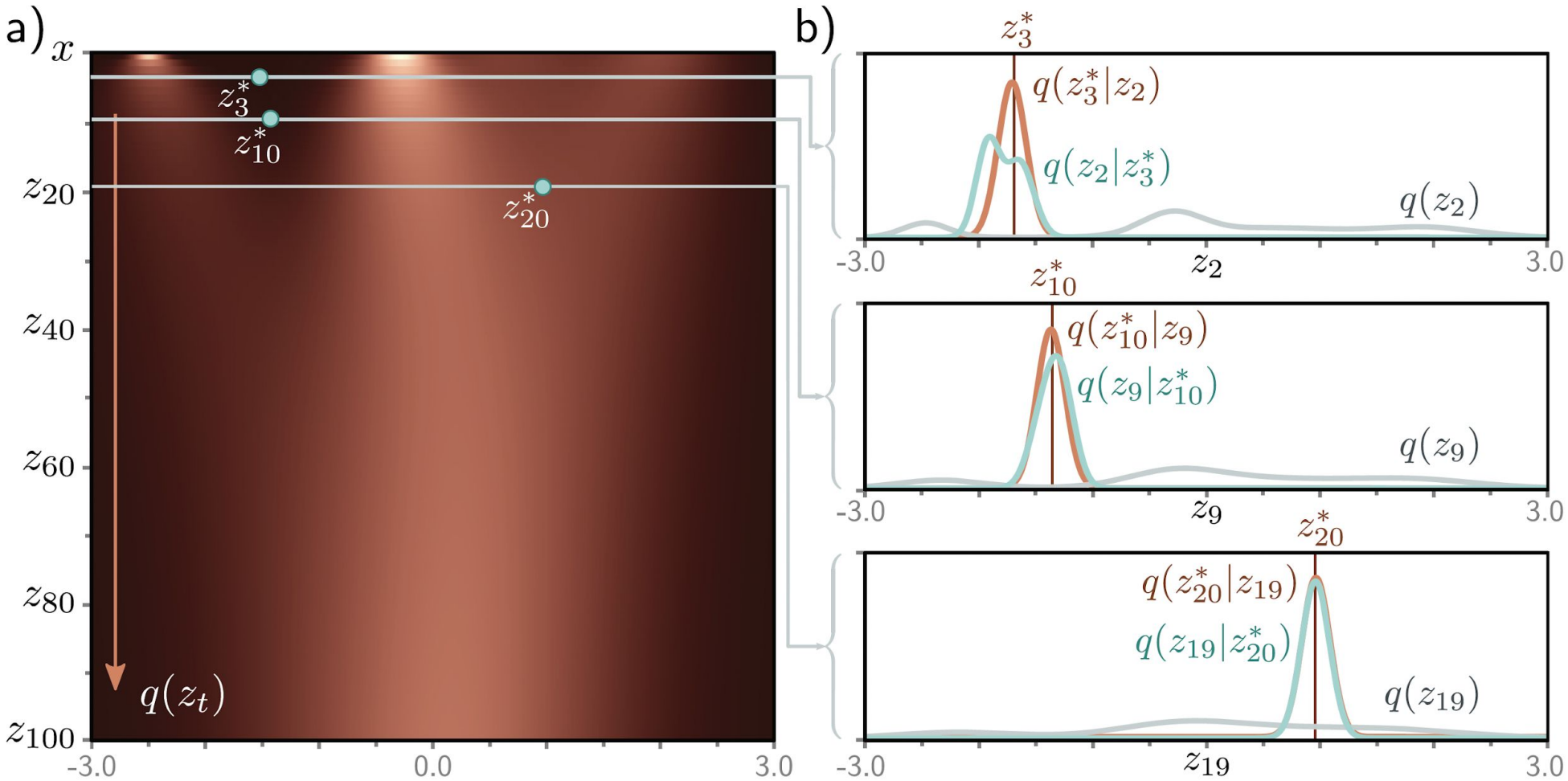

Figure 18.5 Conditional distribution $q(z_{t-1}|z_t)$. a) The marginal densities $q(z_t)$ with three points z_t^* highlighted. b) The probability $q(z_{t-1}|z_t^*)$ (cyan curves) is computed via Bayes' rule and is proportional to $q(z_t^*|z_{t-1})q(z_{t-1})$. In general, it is not normally distributed (top graph), although often the normal is a good approximation (bottom two graphs). The first likelihood term $q(z_t^*|z_{t-1})$ is normal in z_{t-1} (equation 18.2) with a mean that is slightly further from zero than z_t^* (brown curves). The second term is the marginal density $q(z_{t-1})$ (gray curves).

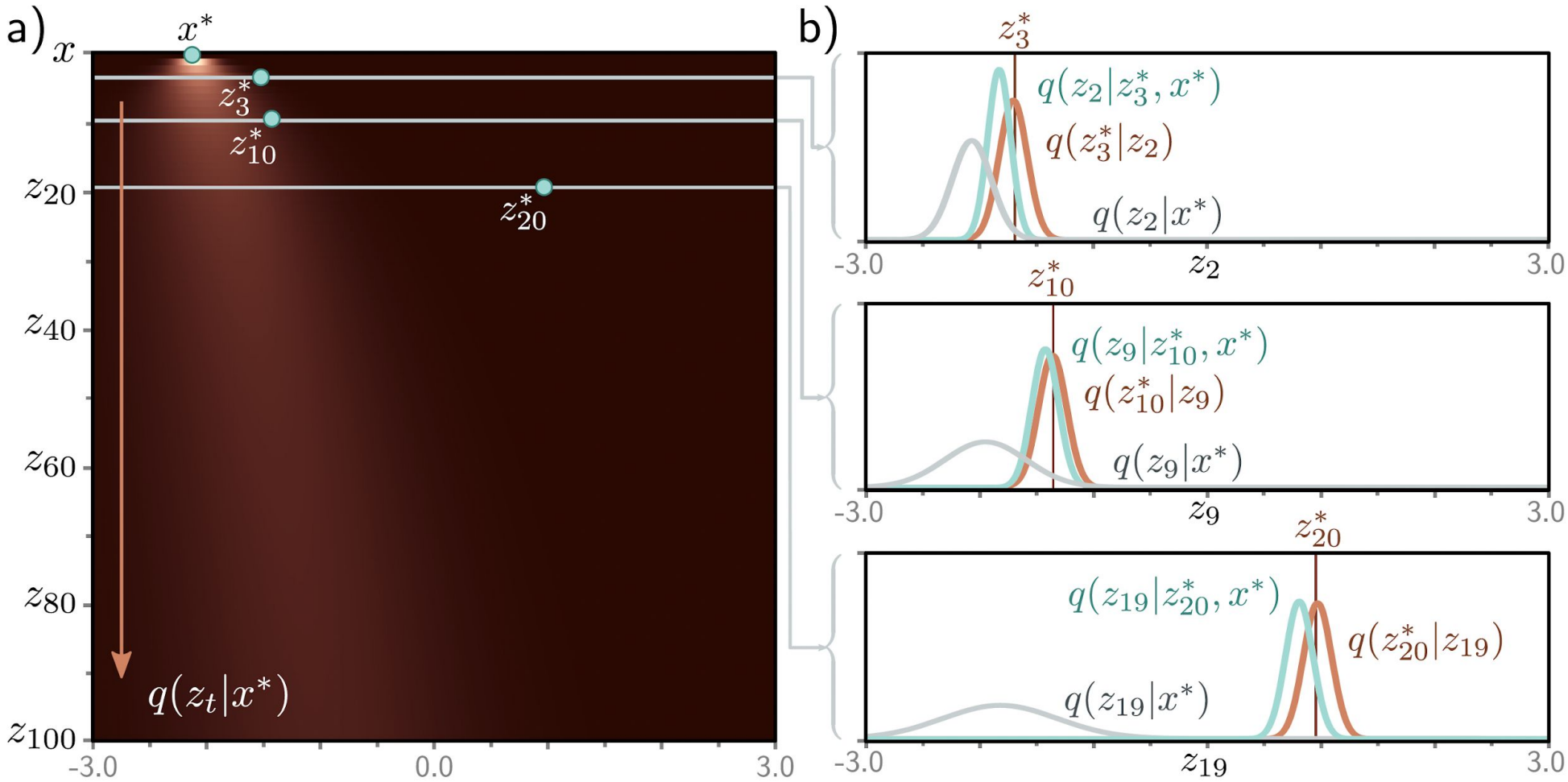

Figure 18.6 Conditional distribution $q(z_{t-1}|z_t, x)$. a) Diffusion kernel for $x^* = -2.1$ with three points z_t^* highlighted. b) The probability $q(z_{t-1}|z_t^*, x^*)$ is computed via Bayes' rule and is proportional to $q(z_t^*|z_{t-1})q(z_{t-1}|x^*)$. This *is* normally distributed and can be computed in closed form. The first likelihood term $q(z_t^*|z_{t-1})$ is normal in z_{t-1} (equation 18.2) with a mean that is slightly further from zero than z_t^* (brown curves). The second term is the diffusion kernel $q(z_{t-1}|x^*)$ (gray curves).

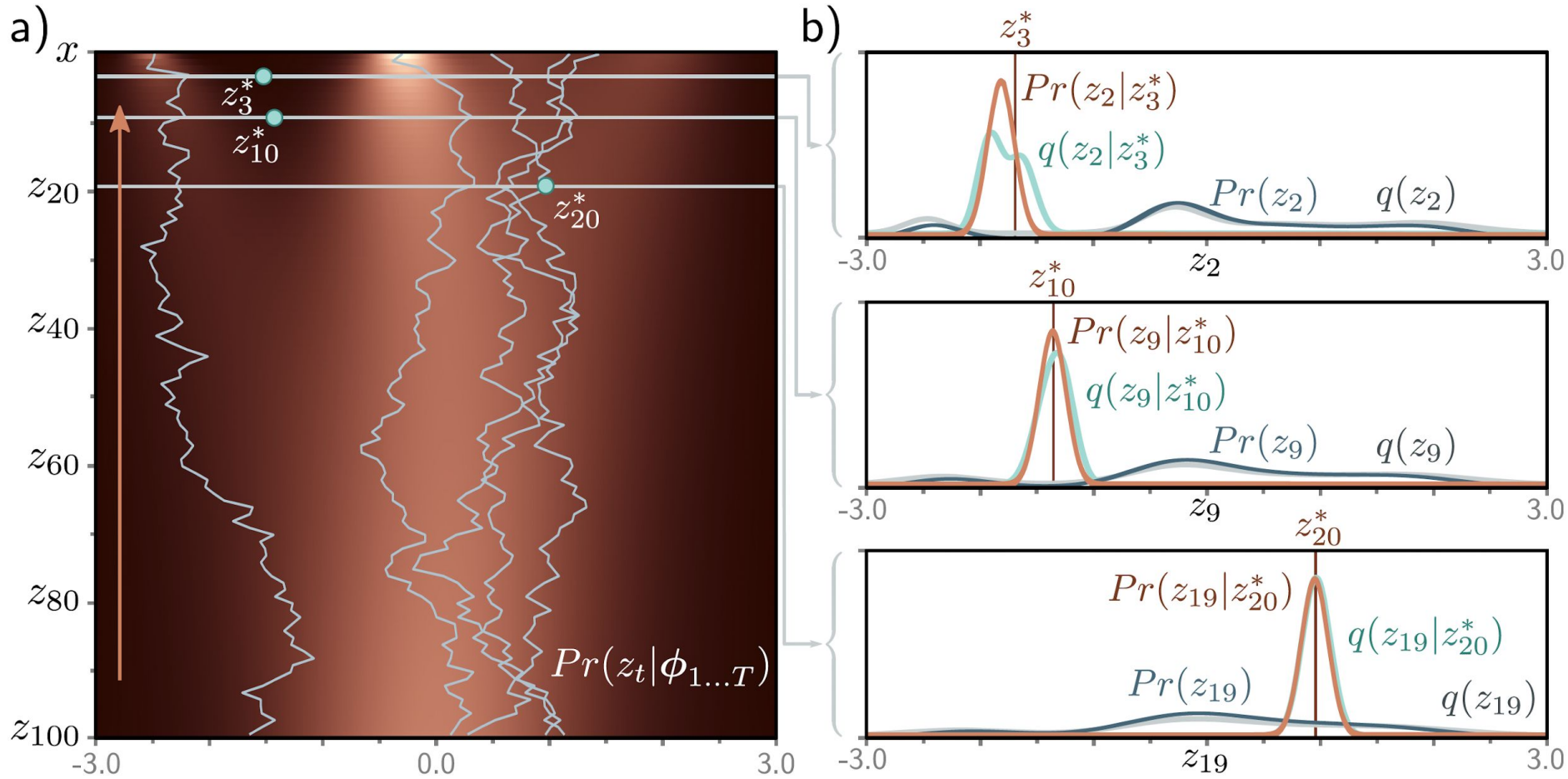

Figure 18.7 Fitted Model. a) Individual samples can be generated by sampling from the standard normal distribution $Pr(z_T)$ (bottom row)and then sampling z_{T-1} from $Pr(z_{T-1}|z_T) = \text{Norm}_{\mathbf{z}_{T-1}}[\text{f}_T[z_T, \boldsymbol{\phi}_T], \sigma_T^2\mathbf{I}]$ and so on until we reach x (five paths shown). The estimated marginal densities (heatmap) are the aggregation of these samples and are similar to the true marginal densities (figure 18.4). b) The estimated distribution $Pr(z_{t-1}|z_t)$ (brown curve) is a reasonable approximation to the true posterior of the diffusion model $q(z_{t-1}|z_t)$ (cyan curve) from figure 18.5. The marginal distributions $Pr(z_t)$ and $q(z_t)$ of the estimated and true models (dark blue and gray curves, respectively) are also similar.

Figure 18.8 Fitted model results. Cyan and brown curves are original and estimated densities and correspond to the top rows of figures 18.4 and 18.7, respectively. Vertical bars are binned samples from the model, generated by sampling from $Pr(\mathbf{z}_T)$ and propagating back through the variables $\mathbf{z}_{T-1}, \mathbf{z}_{T-2}, \ldots$ as shown for the five paths in figure 18.7.

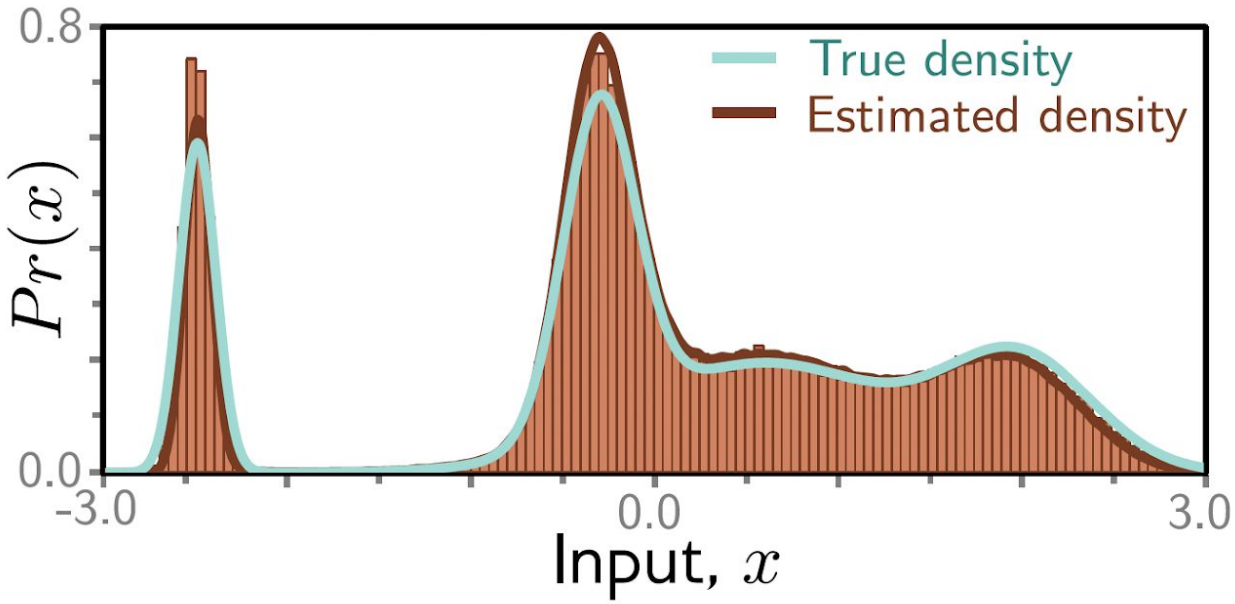

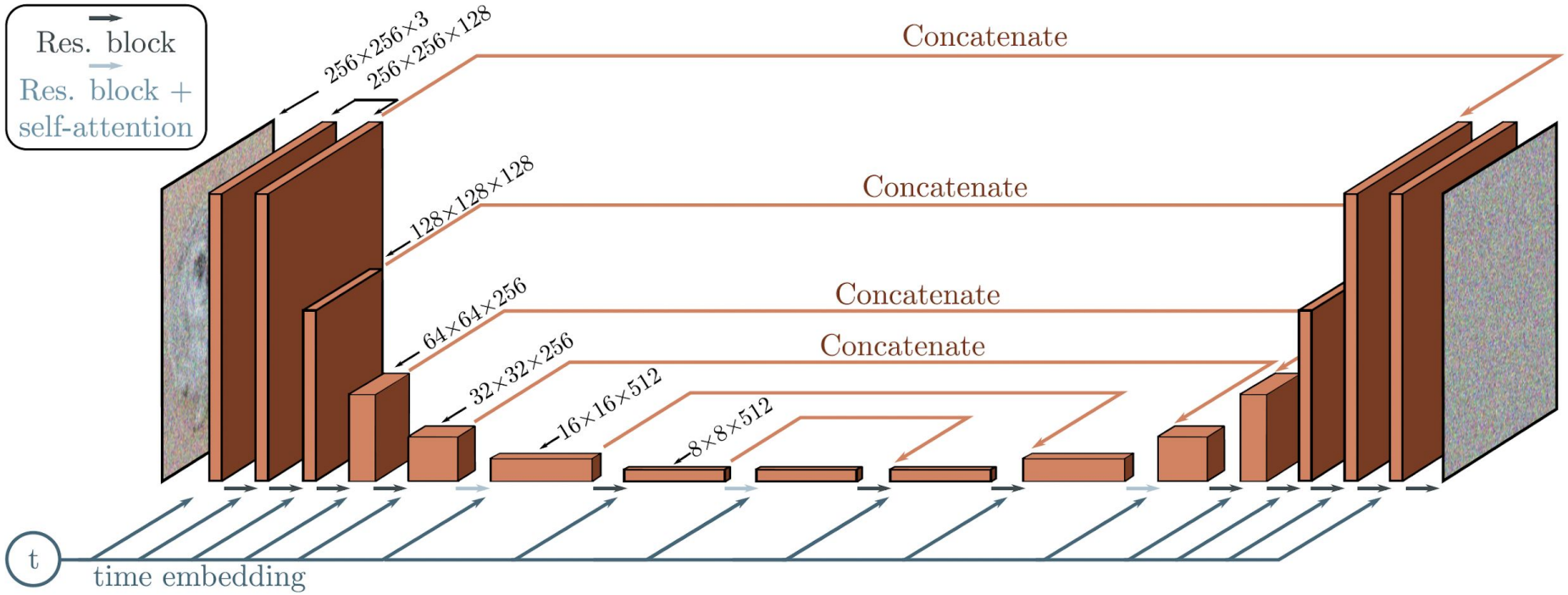

Figure 18.9 U-Net as used in diffusion models for images. The network aims to predict the noise that was added to the image. It consists of an encoder which reduces the scale and increases the number of channels and a decoder which increases the scale and reduces the number of channels. The encoder representations are concatenated to their partner in the decoder. Connections between adjacent representations consist of residual blocks, and periodic global self-attention in which every spatial position interacts with every other spatial position. A single network is used for all time steps, by passing a sinusoidal time embedding (figure 12.5) through a shallow neural network and adding the result to the channels at every spatial position at every stage of the U-Net.

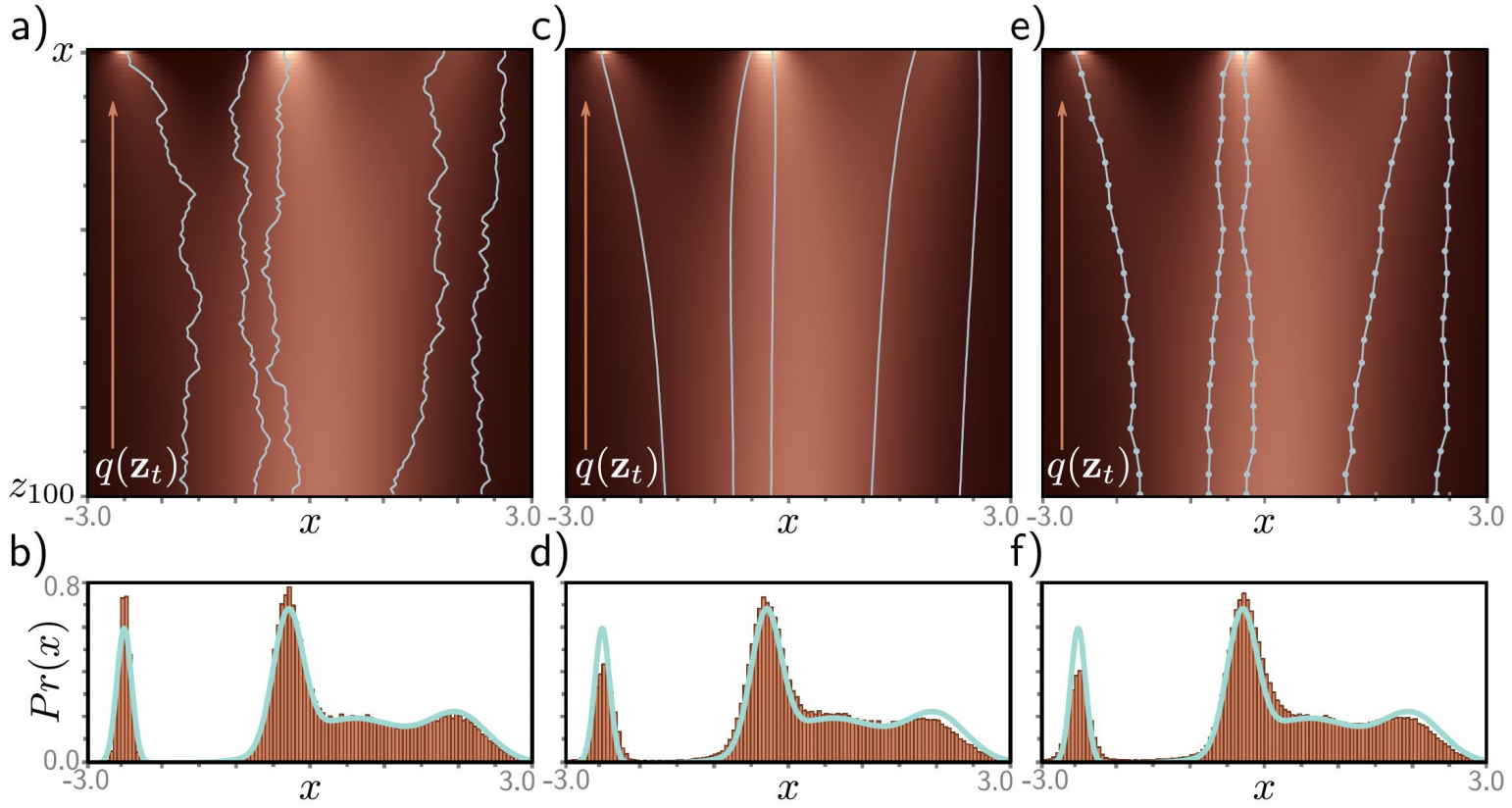

Figure 18.10 Different diffusion processes that are compatible with the same model. a) Five sampled trajectories or reparameterized model superimposed on ground truth marginal distributions. Top row represents $Pr(\mathbf{x})$ and subsequent rows represent $q(\mathbf{x}_t)$. b) Histogram of samples generated from reparameterized model plotted alongside ground truth density curve $Pr(\mathbf{x})$. The same trained model is compatible with a family of diffusion models (and corresponding updates in the opposite direction), including the denoising diffusion implicit (DDIM) model, which is deterministic and does not add noise at each step. c) Five trajectories from DDIM model. d) Histogram of samples from DDIM model. The same model is also compatible with accelerated diffusion models that skip inference steps for increased sampling speed. e) Five trajectories from accelerated model. f) Histogram of samples from accelerated model.

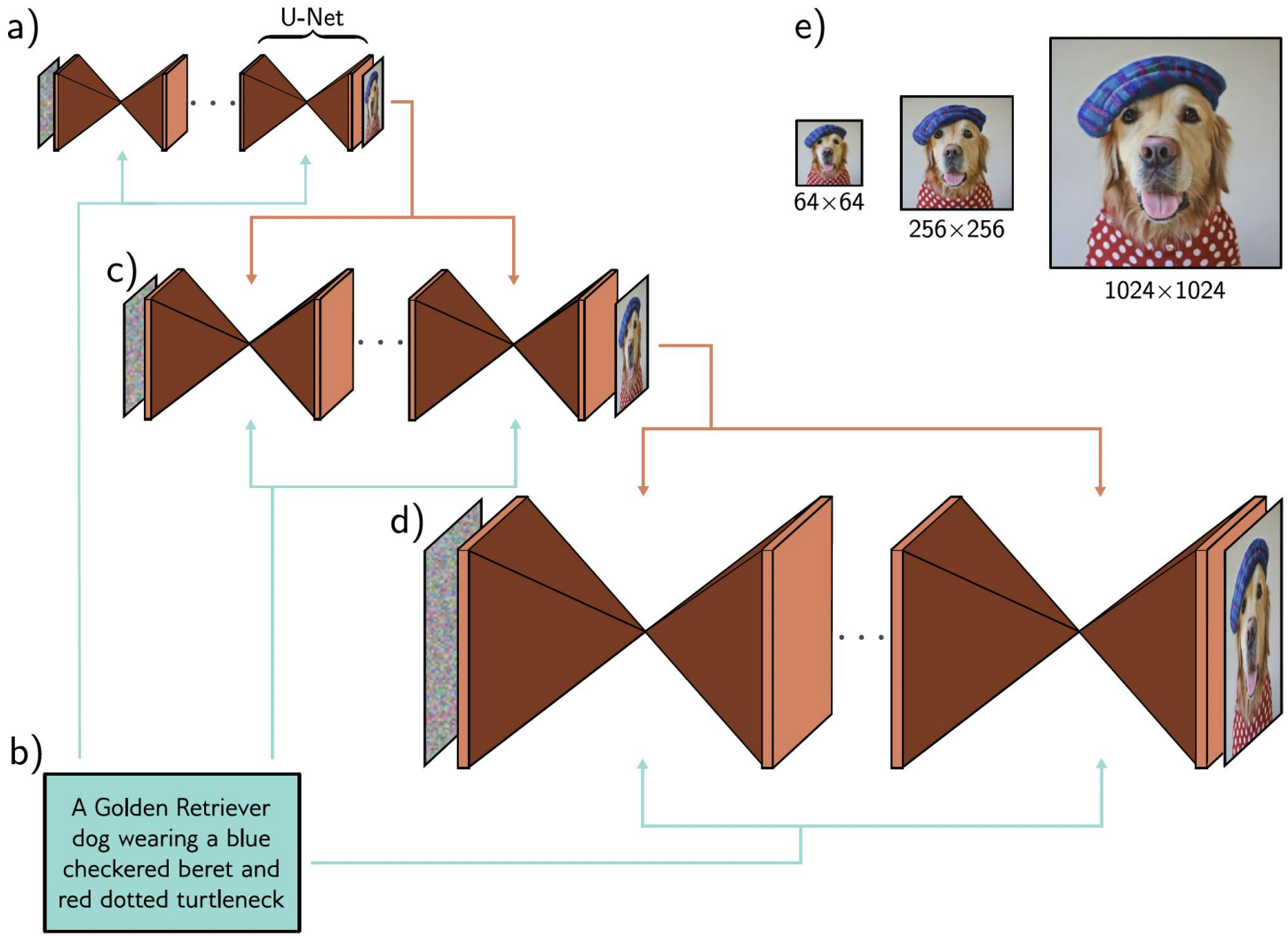

Figure 18.11 Cascaded conditional generation based on a text prompt. a) A diffusion model consisting of a series of U-Nets is used to generate a 64×64 image. b) This generation is conditioned on a sentence embedding computed by a language model. c) A higher resolution 256×256 image is generated and conditioned on the smaller image *and* the text encoding. d) This is repeated to create a 1024×1024 image. e) Final image sequence. Adapted from Saharia et al. (2022b).

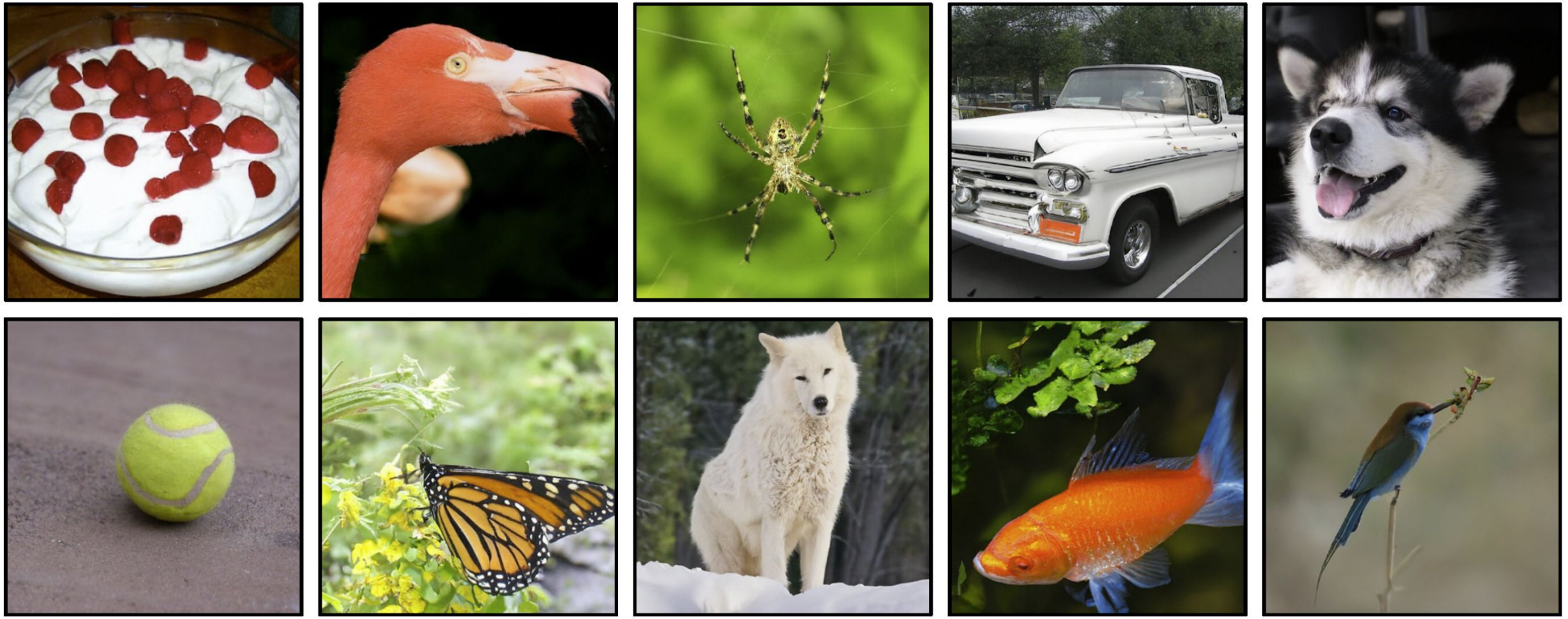

Figure 18.12 Conditional generation using classifier guidance. Image samples conditioned on different ImageNet classes. The same model produces high quality samples of highly varied image classes. Adapted from Dhariwal & Nichol (2021).

Figure 18.13 Conditional generation using text prompts. Synthesized images from a cascaded generation framework, conditioned on a text prompt encoded by a large language model. The stochastic model can produce many different images compatible with the prompt. The model can count objects and incorporate text into images. Adapted from Saharia et al. (2022b).